Negative index Clarricoats-Waldron waveguides for terahertz and far infrared applications

Alessandro Salandrino,* and Demetrios N. Christodoulides,

CREOL/College of Optics and Photonics, University of Central Florida, Orlando Florida 32816, USA
**asalan@creol.ucf.edu*

Abstract: We explore a class of dielectrically loaded metallic waveguides capable of supporting negative index modes in the far infrared and terahertz regime. Principles of operation, modal structure and appropriate coupling schemes are analytically and numerically investigated. The extreme simplicity of the proposed design, along with the non-conventional and counter intuitive electromagnetic properties of this family of waveguides, makes these structures excellent candidates for the practical realization of negative index far infrared and terahertz devices with new and interesting functionalities. Generalizations and extensions of the suggested design are also discussed.

OCIS codes: (230.7370) Waveguides; (260.3090) Infrared, far; (160.3918) Metamaterials.

References and links

1. V. G. Veselago, "The electrodynamics of substances with simultaneously negative values of ε and μ," Sov. Phys. Usp. **10**, 509 (1968) (published in Russian in 1967).
2. D. R. Smith, W. J. Padilla, D. C. Vier, S. C. Nemat-Nasser, and S. Schultz, "Composite medium with simultaneously negative permeability and permittivity," Phys. Rev. Lett. **84**(18), 4184–4187 (2000).
3. J. B. Pendry, A. J. Holden, D. J. Robbins, and W. J. Stewart, "Magnetism from conductors and enhanced nonlinear phenomena," IEEE Trans. Microw. Theory Tech. **47**(11), 2075–2084 (1999).
4. O. Siddiqui, M. Mojahedi, and G. V. Eleftheriades, "Periodically loaded transmission line with effective negative refractive index and negative group velocity," IEEE Trans. Antenn. Propag. **51**(10), 2619–2625 (2003).
5. V. M. Shalaev, "Optical negative-index metamaterials," Nat. Photonics **1**(1), 41–48 (2007).
6. G. V. Eleftheriades, A. K. Iyer, and P. C. Kremer, "Planar negative refractive index media using periodically L-C loaded transmission lines," IEEE Trans. Microw. Theory Tech. **50**(12), 2702–2712 (2002).
7. P. J. B. Clarricoats, and R. A. Waldron, "Non-periodic slow-wave and backward-wave structures," Electron. Control **8**, 455 (1960).
8. R. E. Collin, *Field Theory of Guided Waves*, 2nd ed., (New York, IEEE Press, 1991) Chap. 9: periodic structures.
9. P. J. B. Clarricoats, "Backward waves in waveguides containing dielectrics," Proc. IEE **108**, 496–501 (1961).
10. P. J. B. Clarricoats, and A. B. Birtles, "Circular Waveguide Backward-wave Experiments," J. Electron Contr. **15**, 325–330 (1963).
11. R. A. Waldron, "Theory and potential applications of backward-waves in non-periodic inhomogeneous waveguides," Proc. IEE **111**, 1659–1667 (1964).
12. M. Ibanescu, S. G. Johnson, D. Roundy, C. Luo, Y. Fink, and J. D. Joannopoulos, "Anomalous dispersion relations by symmetry breaking in axially uniform waveguides," Phys. Rev. Lett. **92**(6), 063903 (2004).
13. G. N. Tsandoulas, "Propagation in Dielectric-Lined Square Waveguides," IEEE Trans. Microw. Theory Tech. **23**(5), 406–410 (1975).
14. K. Okamoto, *Fundamentals of Optical Waveguides*, (Academic Press, New York, 2000), Chap. 3: optical fibers.
15. C. S. Lee, S. W. Lee, and S. L. Chuang, "Plot of Modal Field Distribution in Rectangular and Circular Waveguides," IEEE Trans. Microw. Theory Tech. **33**(3), 271–274 (1985).
16. E. F. F. Gillespie, "Power flow and negative impedance in the dielectric rod waveguide," Proc. Inst. Electr. Eng. **107c**, 198–201 (1960).
17. S. Mokhov, R. El-Ganainy, and D. N. Christodoulides, "Power circulation via negative energy-flux wormholes in optical nanowaveguides," Opt. Express **14**(8), 3255–3262 (2006).
18. P. H. Bolivar, M. Brucherseifer, J. Gómez Rivas, R. Gonzalo, I. Ederra, A. L. Reynolds, M. Holker, and P. de Maagt, "Measurement of the Dielectric Constant and Loss Tangent of High Dielectric-Constant materials at Terahertz Frequencies," IEEE Trans. Microw. Theory Tech. **51**(4), 1062–1066 (2003).
19. R. F. Potter, "Germanim (Ge)," in *Handbook of Optical Constants of Solids,* E.D. Palik, ed., (Academic, Orlando, Fla., 1985).
20. S. H. Nam, A. J. Taylor, and A. Efimov, "Subwavelength hybrid terahertz waveguides," Opt. Express **17**(25), 22890–22897 (2009).

#122207 - $15.00 USD Received 4 Jan 2010; revised 1 Feb 2010; accepted 1 Feb 2010; published 4 Feb 2010

1. Introduction

The concept of negative index of refraction dates back to 1967, when Veselago [1] theoretically investigated the electrodynamics of a hypothetical medium having a negative dielectric permittivity and a negative magnetic permeability. In 2000, the first realization of a synthetic negative index medium was reported in the microwave regime [2]. This observation ushered a new area of intense research in both physics and engineering.

In the quest for the realization of negative index materials at ever higher frequencies, two main approaches emerged: one based on modifying the electromagnetic properties of a medium by means of distributed inclusions with appropriate electric and magnetic polarizabilities-such as split ring resonators [3], the other based on the anomalous dispersion of specific guiding configurations in which phase and group velocities are antiparallel [4]. While the first approach could in principle lead to isotropic negative index bulk media, the challenges in practically realizing such systems with current fabrication technologies are severe if not even prohibitive at shorter wavelengths. Indeed the only structures so far realized for the IR and the optical domains are based on few layers of inclusions [5].

On the other hand, while probably not providing the same degree of versatility, waveguide geometries supporting backward modes could represent a more practical avenue for the realization of local negative index environments. Negative index transmission lines were thoroughly investigated [6] and demonstrated in microwave strip line geometries [4] shortly after the first experiments on negative refraction in synthetic bulk media. Although extremely attractive for their ease of fabrication, the inductive loads necessary for the operation of such backward mode transmission lines pose severe challenges when extending these technologies to higher frequencies.

Interestingly, negative index behavior was in fact observed in waveguide configurations by Clarricoats and Waldron [7] in 1960, before the "official" introduction of the negative index concept. The microwave structure considered by Clarricoats and Waldron is built around two basic ingredients: (i) a cylindrical metallic waveguide (ii) coaxially loaded with a high permittivity rod. Even though is well known that backward wave propagation is possible in periodic waveguides [8], this inhomogeneous waveguide system is quite unique in that it may support backward modes, in spite of the fact that the structure is uniform in the propagation direction.

The geometrical conditions ensuring the existence of backward modes were originally studied by the same authors in [9–11] for circular waveguides. A different perspective on these issues was more recently offered in 2004 by Ibanescu *et al.* in [12], in terms of degeneracy of the modes at cut-off. An extension to square geometries was considered by Tsandoulas [13].

In this work we exploit the principles of operation of the Clarricoats-Waldron arrangement to establish a negative index waveguide design suitable for the terahertz and far infrared spectral regions. The extreme simplicity of the proposed design, along with the non-conventional and counter intuitive electromagnetic properties of this family of waveguides, makes these structures excellent candidates for the practical realization of negative index devices with new and interesting functionalities for the far infrared and terahertz regimes. It is our further goal to provide an intuitive understanding of the mechanisms behind the emergence of the anomalous dispersion and ultimately of the negative index behavior. We will show in fact that the origin of the aforementioned effects lies in a local reversal of the Poynting vector due to the convective structure of the magnetic field.

2. Field analysis of the Clarricoats-Waldron waveguide

An idealized structure is presented here in order to isolate the physical mechanisms leading to the unusual electromagnetic properties of the Clarricoats-Waldron waveguide. Therefore in this specific example only lossless dielectrics and perfect electric conductors are considered to first order.

#122207 - $15.00 USD Received 4 Jan 2010; revised 1 Feb 2010; accepted 1 Feb 2010; published 4 Feb 2010

The cross section of a circular Clarricoats-Waldron waveguide is shown in the inset of Fig. 1. A hollow perfect conductor (yellow cylindrical shell) with an internal radius of 31.7μm is loaded with a coaxial dielectric rod of permittivity ε_r = 30 and radius 24.9μm (grey cylinder), surrounded by another (empty in this case) dielectric region. Such geometry is advantageous since all the fields can be computed analytically, in very much the same way as done for ordinary optical fibers [14], with the sole difference that now the tangential electric fields have to vanish at the metallic boundary.

Following the prescriptions of [9–12], the structure was designed so as to induce degeneracy at cut-off of the first two modes. The dispersion curve shown in Fig. 1 illustrates the frequency behavior of the propagation constant β. Under these design conditions the highlighted region of negative group velocity ($dk_0/d\beta$) emerges for the fundamental mode ($k_0 = \omega/c$). As a consequence the power flow and the phase velocity become antiparallel, in other words the mode exhibits negative effective index.

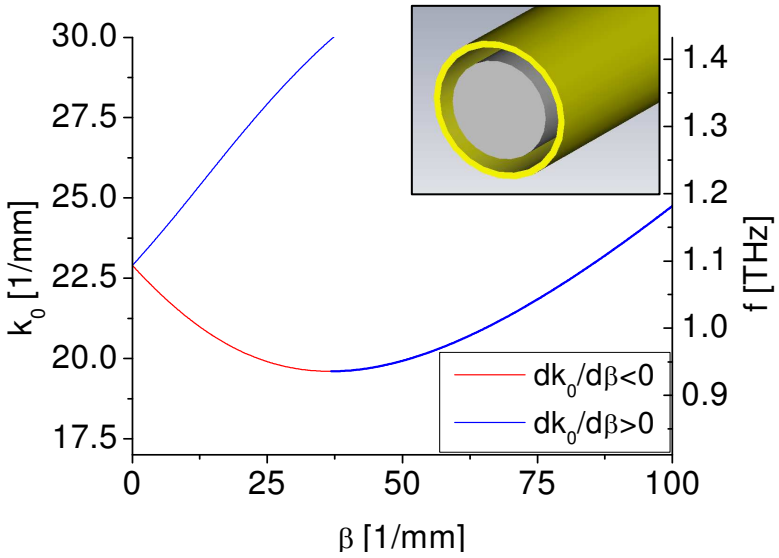

Fig. 1. Dispersion curve of the circular Clarricoats-Waldron guide shown in the inset. The region of negative effective index is shown in red.

Physical insight about the operation of the Clarricoats-Waldron guide may be gained by analyzing in detail the field distributions leading to the anomalous behavior of this structure. Due to the dielectric discontinuity within the guide, the supported modes are necessarily hybrid. In particular, the fundamental mode is a mixture of the TE_{11} and TM_{11} modes of a circular metallic waveguide [15]. The electric and magnetic field distributions of the fundamental backward mode at 1THz are shown in Fig. 2. Interestingly enough, the electric field is reminiscent of the TE_{11} mode, while the magnetic field retains the symmetry of the TM_{11} mode.

The reversal of the magnetic lines of force around the two convective regions visible in the right panel of Fig. 2 and Fig. 3 causes the Poynting vector to change sign and become negative for radial positions external to the centers of the vortices. This, along with the enhancement of the normal component of the electric field in the low permittivity region (due to continuity of the electric displacement at the strong dielectric discontinuity), generates a large negative power flow that overcomes in magnitude the positive flow of the inner core.

#122207 - $15.00 USD Received 4 Jan 2010; revised 1 Feb 2010; accepted 1 Feb 2010; published 4 Feb 2010

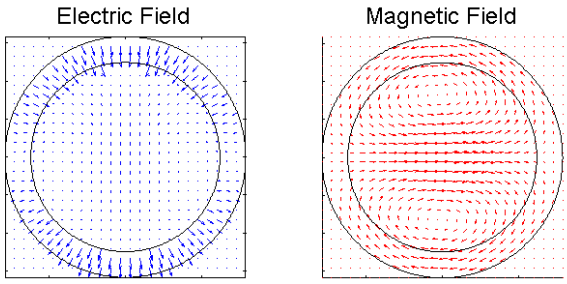

Fig. 2. Electric and magnetic field distribution of the fundamental backward mode in a circular Clarricoats-Waldron guide with dielectric contrast 30, operating a 1THz.

The changing balance between positive and negative power flow induces the non-monotonic concave behavior of the frequency dispersion curve shown in Fig. 1. When the negative power flow equals exactly the positive power flow, the dispersion curve attains an absolute minimum and the group velocity vanishes. Interestingly enough at any given frequency within the backward wave operation bandwidth, a degenerate orthogonal forward solution is always present ("blue" branch). The Poynting vector distributions of a backward mode ("red" branch) and the degenerate forward mode are shown in Fig. 3. along with the corresponding magnetic field lines. The regions of negative power flow are indicated in blue.

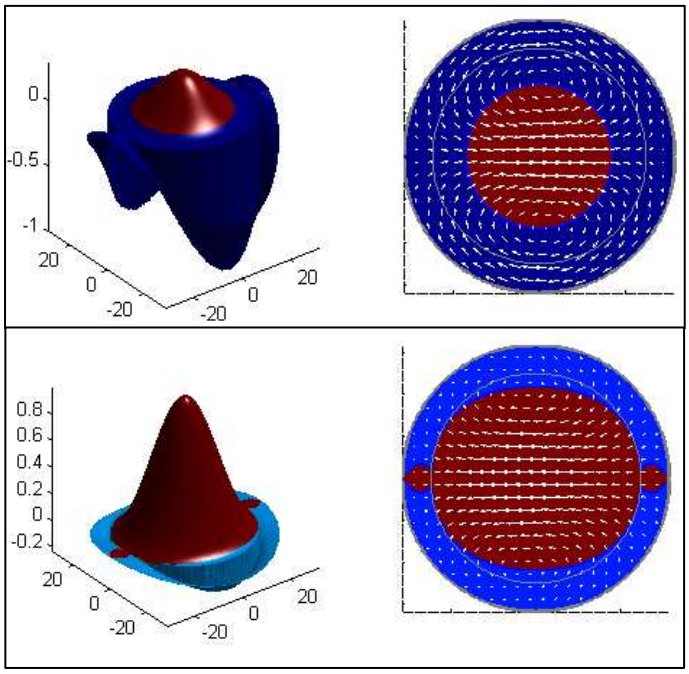

Fig. 3. (left panel) Normalized Poynting vector distribution over a cross section of a Clarricoats-Waldron guide with dielectric contrast 30, operating at 1THz. The regions of positive power flow are indicated in red, while the regions of negative power flow are indicated in blue. (right panel) the magnetic field is shown along with the regions of positive and negative flow. The dielectric interface is shown in gray.

We note that regions of such power flow reversal are also possible in high-contrast dielectric waveguides [16,17]. The selective excitation of the two degenerate modes is discussed in the next section.

#122207 - $15.00 USD Received 4 Jan 2010; revised 1 Feb 2010; accepted 1 Feb 2010; published 4 Feb 2010

3. THz design of a Clarricoats-Waldron guide

In this section we present and analyze a design suitable for THz applications. Considering the fact that high permittivity low loss ceramic materials are nowadays available in the THz band [18], the original circular coaxial layout of the Clarricoats-Waldron waveguide could be in principle scaled down to operate in the THz regime. Nevertheless the practical realization of such circular geometry for THz applications, due to the small dimensions and the free standing central dielectric rod, could pose severe challenges from the fabrication point of view.

An important simplification of the original design may be achieved by considering the symmetry of the first backward mode. Due to the cosine azimuthal dependence of the electric field it is possible to replace half of the structure by an electric ground plane, while preserving all the boundary conditions and leaving the electromagnetic behavior unaffected. The resulting geometry in a half-square configuration is presented in Fig. 4(a). The field distribution and the dispersion curve shown in Fig. 4(b) were computed with the commercial finite elements software Comsol Multiphysics™.

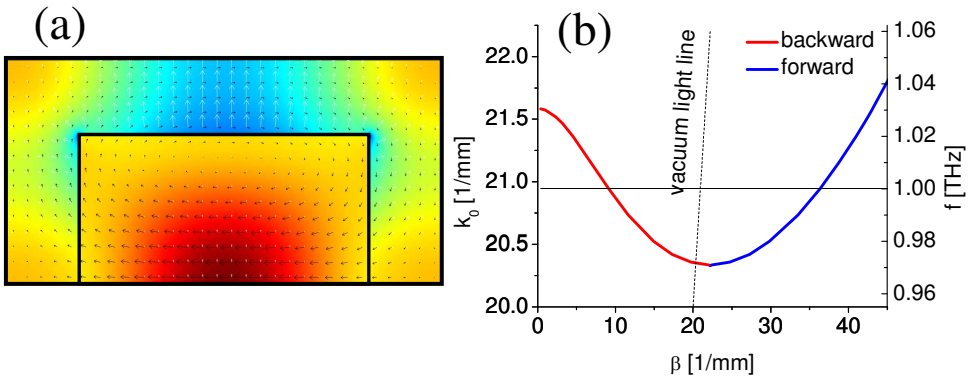

Fig. 4. (a) Numerical simulation of power flow and field distribution in a Clarricoats-Waldron rectangular waveguide of dimensions 80μm x 40μm, loaded with a Germanium rod of dimensions 53μm x 26.5μm, operating at 1THz . (b) Dispersion relation.

For this specific design a rectangular hollow waveguide made of gold and loaded with a germanium rectangular rod is considered. The complex permittivity of Ge [19] at this frequency is 16.04 + i*0.016. The skin depth of gold is estimated based on a Drude model [20] to be less than $2x10^{-5}$cm. The dimensions are chosen to be 80μm x 40μm for the metallic wall and 53μm x 26.5μm for the dielectric load, so as to achieve backward wave operation around 1THz. Based on these design parameters the field decay constant of the fundamental backward mode at 1THz is perturbatively estimated to be $\alpha = 0.37 cm^{-1}$.

A very important issue to be addressed is the selective excitation of only the backward mode. Given the orthogonality of the modes, one possibility is certainly the excitation at a waveguide cross-section with the exact field distribution matching the mode structure. A far more straightforward solution may be obtained by observing the dispersion curve in Fig. 4(b).

Even though the forward and backward solutions are degenerate in frequency, their wave-vectors are significantly different, so a properly phase matched field could effectively excite through a slit only one of the modes. Furthermore the vacuum light line in Fig. 4(b) shows that the phase velocity of the backward mode is mostly superluminal, while the phase velocity of the forward mode is always subliminal. As a consequence the backward mode and the backward mode only could be excited through a slit by an external homogeneous plane wave. This can be done in a distributed manner from a standard waveguide-through an arrangement resembling that of a distributed feedback structure. As a further remark, this coupling

#122207 - $15.00 USD Received 4 Jan 2010; revised 1 Feb 2010; accepted 1 Feb 2010; published 4 Feb 2010

approach could lead to the realization of waveguide couplers with non conventional routing properties.

4. Generalizations and extensions: Clarricoats-Waldron arrays

As pointed out in the previous paragraph, one of the obstacles towards the extension of the Clarricoats-Waldron design to higher frequencies is the need for an ideal metal to enclose the structure. A solution to this problem may be found by considering an array of identical square guides excited with the same mode. It is straightforward, by invoking the principle of images, to prove that all of the internal walls separating the single elements may be removed without affecting the field distribution. The numerical simulations of the field distribution for a single element and for a 2D array of 9 elements are shown in Fig. 5. As evident, each single element retains the field configuration of the structure in isolation.

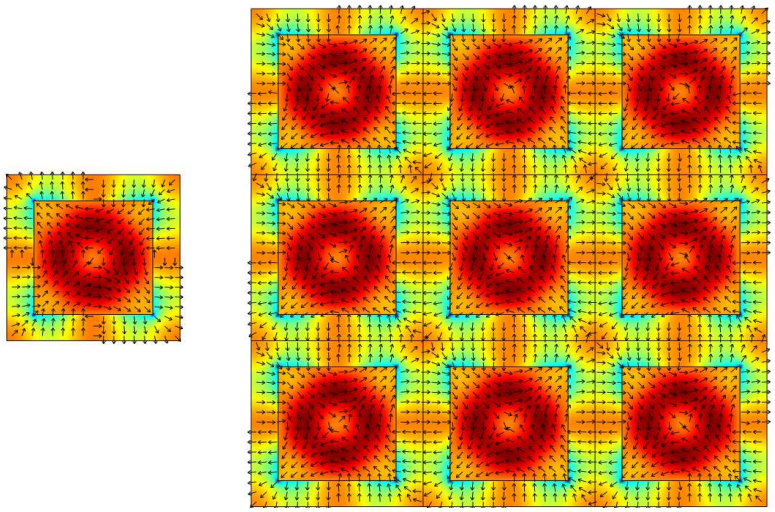

Fig. 5. Power flow and electric field distribution in a single element and in a 2D Clarricoats-Waldron array.

The behavior shown in Fig. 5 is a consequence of the symmetry of both the structure and the excitation. The modal configuration of the isolated element is fully retained only by the super-mode with in-phase excitation of the elements. The more complex behavior of higher order super-modes will be the subject of further investigations.

5. Conclusions

A new class of THz and far infrared waveguides capable of supporting negative index modes was proposed. The working mechanisms were clarified in terms of their modal properties. A suitable design for THz operation was proposed and numerically analyzed. The simple geometry of the Clarricoats-Waldron waveguide makes these structures versatile tools for the study of phenomena related to negative index and backward-wave propagation in the THz domain. The original design was generalized to array geometry as a possible avenue to extend the applicability of these components in the mid-IR regime.

#122207 - $15.00 USD Received 4 Jan 2010; revised 1 Feb 2010; accepted 1 Feb 2010; published 4 Feb 2010